JOURNAL OF MATERIALS SCIENCE **36** (2001) 2441–2449

# The oxidation of SiC particles and its interfacial characteristics in Al-matrix composite

ZHONGLIANG SHI
*State Key Laboratory of Metal Matrix Composites, Shanghai Jiao Tong University, Shanghai 200030, People's Republic of China; Mesoscopic Materials Research Center, Graduate School of Engineering, Kyoto University, Kyoto 606-8501, Japan*
*E-mail: zlshi@mech.kyoto-u.ac.jp*

SHOJIRO OCHIAI, MASAKI HOJO
*Mesoscopic Materials Research Center, Graduate School of Engineering, Kyoto University, Kyoto 606-8501, Japan*

JAECHUL LEE
*Division of Materials Science and Engineering, Korea Institute of Science and Technology, P.O. Box 131, Cheongryang, Seoul, South Korea*

MINGYUAN GU
*State Key Laboratory of Metal Matrix Composites, Shanghai Jiao Tong University, Shanghai 200030, People's Republic of China*

HOIN LEE
*Division of Materials Science and Engineering, Korea Institute of Science and Technology, P.O. Box 131, Cheongryang, Seoul, South Korea*

RENJIE WU
*State Key Laboratory of Metal Matrix Composites, Shanghai Jiao Tong University, Shanghai 200030, People's Republic of China*

The passive oxidation behavior of SiC particles has been studied in an electric furnace at atmospheric pressure and in dry air, the weight change due to the transformation from SiC into $SiO_2$ is descibed as a function of exposed temperature and holding time. According to the oxidation data of SiC particles, the oxidation parameters and the degree of oxidation for SiC particles can be controlled. Controllable preoxidation of SiC particles is one of the keys for designing interface and interphase to achieve high performance aluminum composite. Consequently, the evolution of interfacial reaction products in 2014 aluminum alloy composite reinforced with oxidized-SiC particles after extended thermal exposure at elevated temperatures were further characterized by Scanning Electron Microscopy (SEM), Transmission Electron Microscopy (TEM), and X-ray diffraction. While it could act to prevent the interfacial reaction between SiC particles and aluminum alloy, the preoxidation of SiC particles led to the formation of other interfacial reaction products. The observation of the microstructure revealed that at elevated temperatures nano-MgO formed initially on the surface of the oxidized SiC particles and then turned into nano-$MgAl_2O_4$ crystal due to the reaction between the $SiO_2$ and aluminum alloy containing Mg. TEM observations indicated that the oxidized layer on SiC particles was uniform and had a good bonding with SiC and aluminum alloy. 

## 1. Introduction

The oxidation of SiC materials has been the topic of investigation for many years because of their application at high temperatures. The excellent oxidation resistance which SiC exhibits is due to the formation of a coherent layer of $SiO_2$ on the surface which suppresses further oxidation. Oxidation kinetics can generally be described using the linear-parabolic model at atmospheric pressure and in dry oxygen [1–4]. The passive silica layer, which grows naturally or artificially on the surface of SiC particles or fibers used in aluminum-based composites, is supposed to have two functions: protection of the SiC from aluminum attack and improvement of the wettability of SiC to aluminum which would result from the reaction between aluminum and $SiO_2$ [5–7].

In the case of aluminum matrix composites reinforced with SiC as reinforcement either its fiber or

particle, the reaction results in the formation of $Al_4C_3$ at the interface:

$$4Al + 3SiC \rightarrow Al_4C_3 + 3Si \quad (1)$$

$Al_4C_3$ forms as a discontinuous layer (rod-like [8], hexagonal platelet [9, 10]) and hence does not affect the wettability between SiC and molten aluminum alloys significantly. However, the formation of $Al_4C_3$ degrades the particles and the fibers, resulting in poor mechanical properties of composites. Therefore, during the composite fabrication, three primary techniques have been employed for controlling the deleterious interfacial reactions. (1) Modification of matrix chemical composition. For example, in SiC/Al composites, Si was added into the aluminum alloy matrix in order to hinder the above interfacial reaction. Lee *et al*. [11] clarified theoretically the equilibrium Si contents required to prevent the formation of $Al_4C_3$ in SiC/Al composites, by taking into account the variations in Al and Si activities as well as those of other compounds in the calculations. (2) Control of the processing parameter so as to limit the extent of the interfacial reaction. Examples are controlling the processing temperature and holding time during composite fabrication. Thereby, the various composite processing methods such as compocasting, squeeze casting, semisolid forming (thixoforming), spray forming, and powder metallurgy can be used for the composite fabrication [12–14]. (3) Surface modification of reinforcement by coating or passive oxidation. This technique has been successful to some extent in preventing the detrimental interfacial reaction and enhancing the materials wettabilities. Warrier *et al*. [15, 16] reported that copper and silver coating had significantly promoted the wettability of the C and SiC fibers with molten aluminum alloys. Among the techniques mentioned above, (3) especially the preoxidation of SiC is considered to have high potential for practical fabrication. The purpose of the present work was to clarify the degree of oxidation of SiC particles and to observe their surface morphology and the interfacial characteristics of oxidized SiCp reinforced 2014 Al composite.

## 2. The theoretical background on oxidation of SiC particles

As known, when SiCp is oxidized and formed vitreous $SiO_2$, one mole SiC is oxidized completely into the same mole $SiO_2$, the weight gain per mole is theoretically 20 g because of the difference of their molecular weights. Thus if $x$ weight of SiC (g) is oxidized to form $y$ (g) weight of $SiO_2$, then the relationship between $x$ and $y$ is given by Equation 2 through the chemical reaction equations given by Equation 3.1–3.3

$$y = 1.5x \quad (2)$$

$$SiC + O_2 \rightarrow SiO_2 + C \quad (3.1)$$

$$2SiC + 3O_2 \rightarrow 2SiO_2 + 2CO \quad (3.2)$$

$$SiC + 2O_2 \rightarrow SiO_2 + CO_2 \quad (3.3)$$

Actually the mole of SiC is transformed into the same mole vitreous $SiO_2$ as seen from all reaction equations mentioned above. In the following calculation, equation (3.3) is adopted representatively since the oxidation is carried out at air atmosphere for long time. Even if other reaction equations are used, the conclusion is the same.

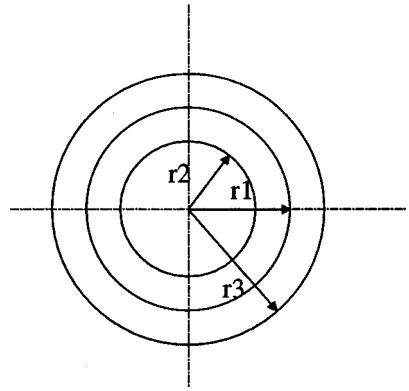


*Figure 1* The schematic of the change of SiC particle after oxidation.

The data of weight gain ($\Delta w$) obtained from the data collection of the computer equals to the equation $\Delta w = y - x$, which will change with temperature and time. The weight of the oxidized SiC and $SiO_2$ can be calculated to be $x = 2\Delta w$ and $y = 3\Delta w$, respectively. The densities of SiC and the vitreous $SiO_2$ are $\rho_{SiC} = 3.16$ and $\rho_{SiO_2} = 2.196$ [17], the volume fractions of $SiO_2$ formed by oxidation can be calculated by Equation 4.

$$V_{SiO_2} = \frac{\dfrac{y}{\rho_{SiO_2}}}{\dfrac{W-x}{\rho_{SiC}} + \dfrac{y}{\rho_{SiO_2}}} = \frac{\dfrac{3\Delta w}{\rho_{SiO_2}}}{\dfrac{W-2\Delta w}{\rho_{SiC}} + \dfrac{3\Delta w}{\rho_{SiO_2}}} \quad (4)$$

Assuming the same size of SiC particles and the same shape of spheres, shown as in Fig. 1, the initial diameter of SiC particle is $2r_1$. After it is oxidized partially to from $SiO_2$ , the volume fraction of $SiO_2$ can be calculated by (5):

$$\text{Vol\%}V_{SiO_2} = \left[1 - \left(\frac{r_2}{r_3}\right)^3\right] \times 100\% \quad (5)$$

where $r_2$ is the radius of remained SiC after oxidation. If SiC particle is completely oxidized to form vitreous $SiO_2$, the volume ratio between SiC and $SiO_2$ is given by

$$\frac{V_{SiC}}{V_{SiO_2}} = \left(\frac{r_1}{r_3}\right)^3 = \frac{m_{SiC}/\rho_{SiC}}{V_{SiO_2}/\rho_{SiO_2}} \quad (6)$$

where, $m_{SiC}$ and $m_{SiO_2}$ are the molecular weights of SiC and $SiO_2$, respectively, being $m_{SiC} = 40$, $m_{SiO_2} = 60$. The data of volume of $V_{SiO_2}$ can be calculated by Equation 4. Thus, from Equations 5 and 6, the thickness of $SiO_2$ layer is expressed as (7). Thus, the thickness of oxidized layer $SiO_2$ at the surface of SiC particle can be derived from its weight changes.

$$t = r_3 - r_2 = 1.29r_1\left(1 - \sqrt[3]{1 - \text{ vol\%}V_{SiO_2}}\right) \quad (7)$$

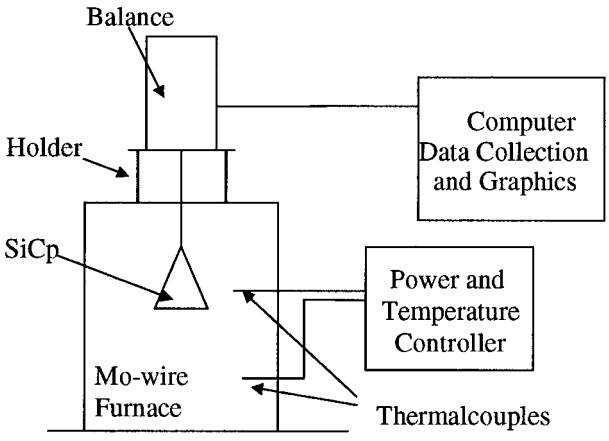


*Figure 2* The schematic for oxidation of SiC particles and its measurement.

## 3. Experimental procedures

### 3.1. The oxidation of SiC particles

SiC particles used in this study were the hexagonal $\alpha$-SiC (6H) and the average size was 5 $\mu$m. The oxidation process of SiC particles was carried out in an electric furnace in air at atmospheric pressure. The alumina crucible (high purity alumina, $Al_2O_3$ content over 99%), in which 10 g SiC particles were loaded, was hung in the furnace using a fine Pt wire. The other end of the wire was connected to the balance. The balance was also connected with the data collection of computer, as shown in Fig. 2. SiC particles were heated to preset temperatures, i.e. 1100°C, 1200°C and 1300°C with a heating rate of 10°C/min with a maximum exposure time of 40 hours. The weight change due to the formation $SiO_2$ during the oxidation was recorded every 4 minutes. The oxidation tests were carried out twice to confirm the accuracy. The oxidation of SiC particles was found to start from 800°C. The weight gains measured from 800°C to preset temperatures were insignificant and could be neglected, compared with the weight gain at the preset temperatures. Using the measured weight change of SiC particles with temperature and time, the volume of $SiO_2$ and its thickness were calculated, based on the procedure in part 2.

### 3.2. The preparation of composites with oxidized SiC particles

The oxidized SiCp/2014Al composite was prepared by infiltrating the commercial 2014 Al melt into pre-oxidized SiC powders. The composition of the 2014 Al was Al-3.9Cu–0.54Si–0.32Mg–0.56Mn (the results from chemical analysis). The particles used for fabrication of the composite were prepared in an artificially oxidized condition at 1100°C for two hours using an alumina crucible heated with Mo-wire furnace. After oxidation, the accumulated particles were ground and sifted with a grid 70 $\mu$m screen. In order to facilitate penetration of the 2014 Al melt through SiC powders, the tool steel die in which the oxidized SiC particles were loaded was preheated to a temperature of 550°C. The 2014 Al alloy which was melt at 760°C in a graphite crucible, was poured into the die and pressurized up to 100MPa with a hydraulic press.

### 3.3. Electrochemically extracted oxidized SiCp/2014 Al composite

Since the size and volume fraction of the interfacial reaction products within the composites were very small and low respectively, the morphology of the embeded particles could not be observed directly. In order to overcome such a problem in observation, the interfacial reaction products as well as ceramic reinforcements were extracted electrochemically from the composite heat-treated at elevated temperatures such as 560°C, 600°C etc for one or two hours. The electrolyte used was 33 vol% $HNO_3$ + 67 vol% water. The voltage and current used for the extraction were 10–15 DC volts and 5–10 Amp, respectively. The electrolyte was maintained at 0–5°C throughout the extraction process. The surfaces of electrochemically etched composites were observed by FE-SEM (Field Emission—Scanning Electron Microscopy, Hitachi S-4200). The interfacial reaction products were identified by x-ray diffraction, which scanned at a rate of 0.01° per 4 sec in a step scan mode using monochromated Cu $K_\alpha$ radiation. The detailed interfacial reaction products were further identified by TEM (JEOL 2010). The TEM specimen was prepared by mechanical grinding and ion milling.

## 4. Results and analysis

### 4.1. The passive oxidation characteristics of SiC particles at elevated temperature

When SiC particles are exposed at the elevated temperatures, the weight of the resultant SiC will increase due to the formation of $SiO_2$ on their surfaces. Fig. 3a shows the variation in the weight of SiC measured as a function of heating temperature and heating preservation time. The parabolic trend of the curves is a good indication that the passive oxidation has occurred during the oxidation of SiCp. This also agrees with the results of the two previous reports [2, 3]. It is noted that, for prolonged holding time, the weight gain at 1200°C approached the value at 1300°C. This trend shows the decline of volume-increasing-rate of $SiO_2$ and the reduction of the weight gain of $SiO_2$ transformed from SiC for prolonged exposure time and the coherent layer of $SiO_2$ which has formed at the surface of SiC particles will suppress further oxidation. The dependence of the volume fraction of $SiO_2$ on the temperature and time is shown in Fig. 3b. The relationship between the thickness of $SiO_2$ layer and the temperature and holding time is also shown in Fig. 3c. It can be noted that the thickness of $SiO_2$ ($= r_3 - r_2$, in Fig. 1) is closed to 1000 nm at the temperature 1300°C and holding about 40 hours; actually the average size of particles after the oxidation at this temperature and holding time are up to 7 $\mu$m (the average size of as-received SiC particles is 5 $\mu$m).

Fig. 4 shows the dependence of volume-increasing-rate of $SiO_2$ on the holding time. It is clearly found that the rates at the different elevated temperatures have great changes only for initial 5 hours of holding time, but then the rates are close at the rest holding time. The result is very important for the selection of the oxidation condition (temperature and time) of SiC particles in fabrication of the composite.

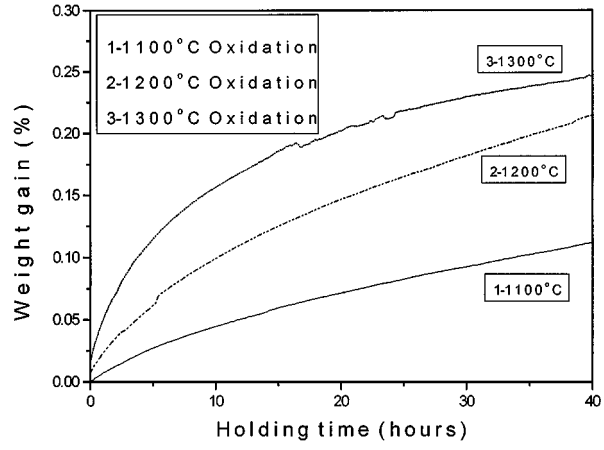


(a)

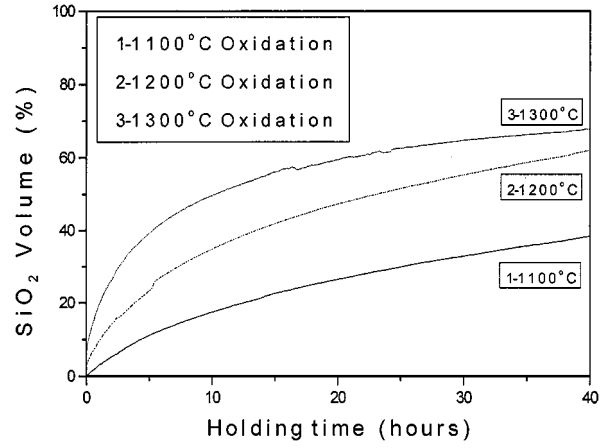


(b)

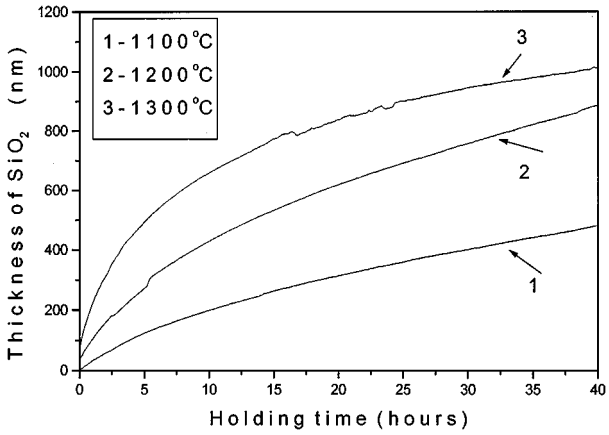


(c)

*Figure 3* (a) The weight gain, (b) the volume fraction of $SiO_2$ layer and (c) thickness of $SiO_2$ layer (nm) as a function of holding time during the oxidation of SiCp at 1100–1300 °C.

## 4.2. Interfacial characteristics of oxidized-SiCp/2014Al composites

In order to observe the morphological evolution of interfacial reaction products and the surface of oxidized SiC particles, the Al matrix was removed electrochemically from the composite. This revealed the oxidized SiC particles as well as the interfacial reaction products. Fig. 5a showed the micrograph of the particles that were extracted from the as-cast composites reinforced with oxidized SiC particles. Its surface was very clean and showed no obvious reaction products during the squeeze cast processing. Fig. 5b shows the HRTEM image of the interfacial region of an as-cast SiCp/2014Al composite with particles oxidized at 1100°C for 2 hours. A uniform $SiO_2$ layer with a thickness of 45–50 nm was observed at the interface. Additional beneficial effects from the oxidation of SiC

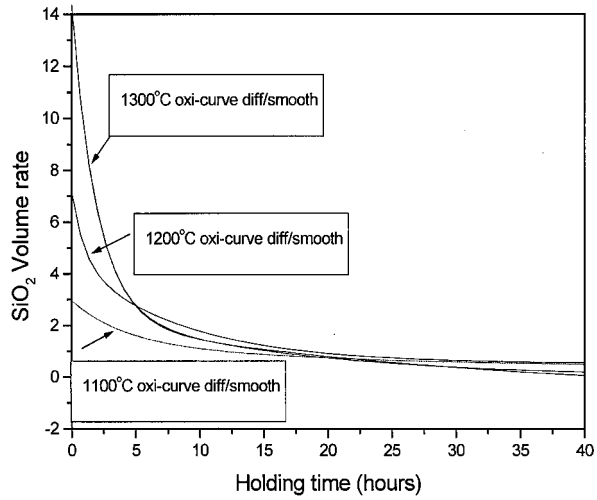


*Figure 4* The dependence of growth of volume rate of $SiO_2$ layer on holding time at elevated temperatures 1100 °C–1300 °C.

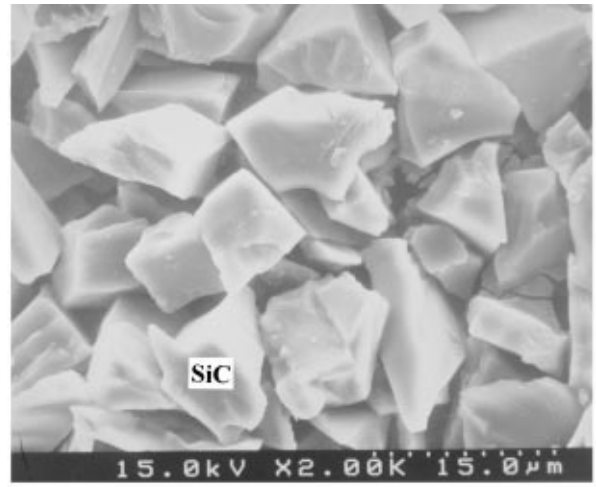


(a)

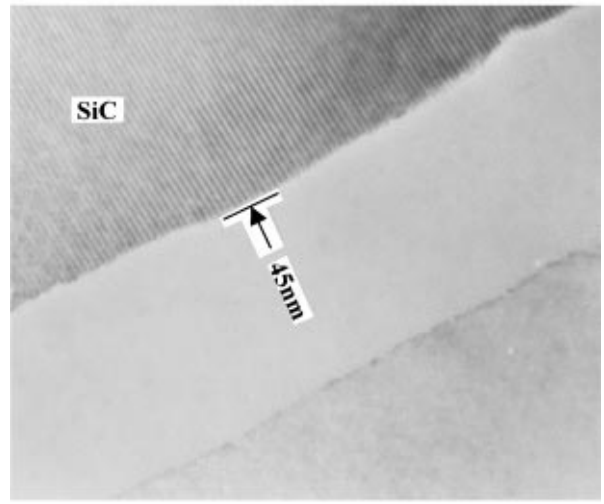


(b)

*Figure 5* (a) SEM micrographs showing the extracted particles and (b) HRTEM image showing the thickness of $SiO_2$ at the surface of oxidized SiC particles from as-cast composites samples: (a) as-cast composite with oxidized particles and (b) the thickness of oxidized layer of the composite reinforced with oxidized SiC particles at 1100°C for 2 hours.

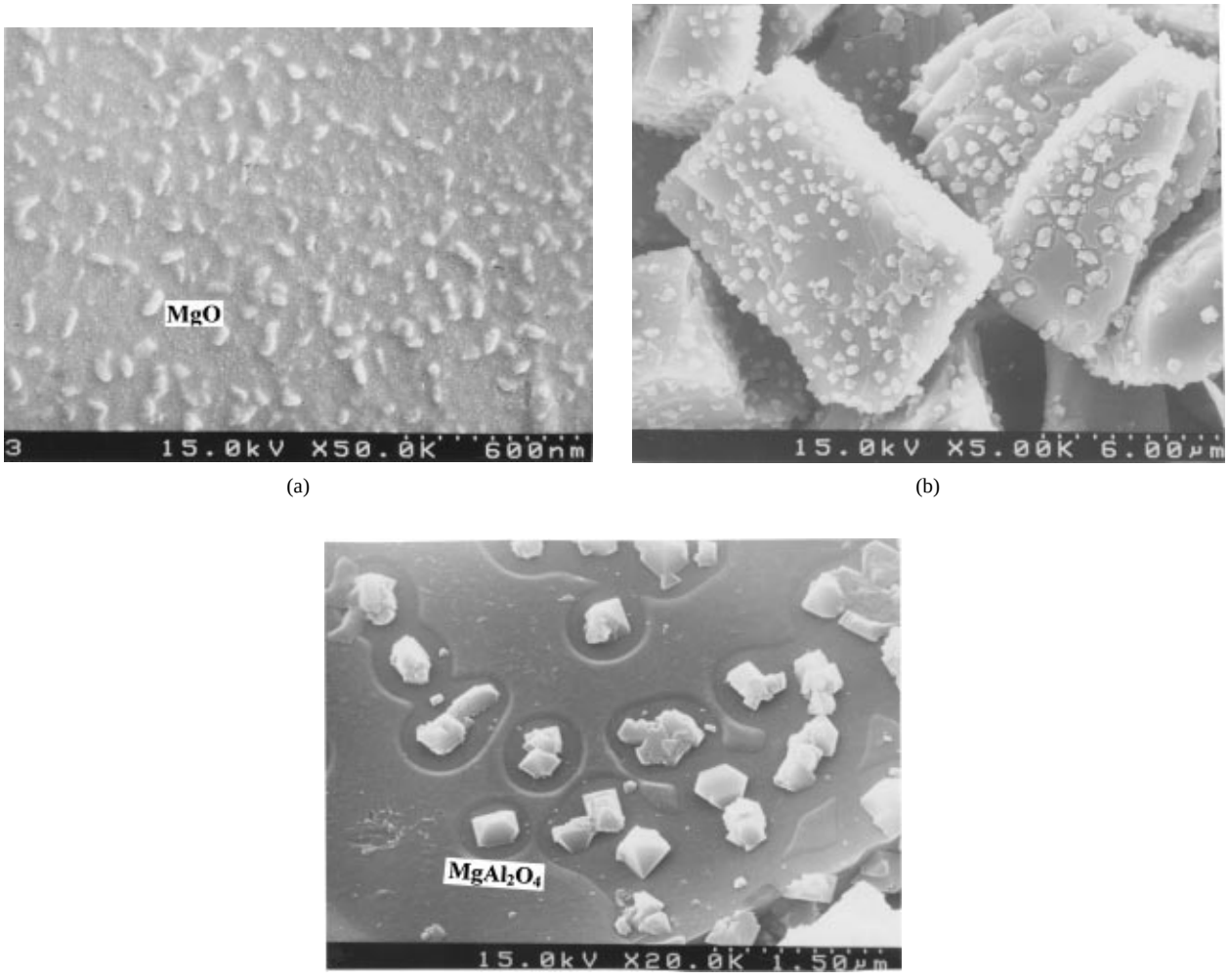


(a) (b)

(c)

*Figure 6* SEM micrographs showing the surface of extracted particles from the composites reinforced with SiC oxidized at 1100°C for 2 hours samples: (a) heat-treated at 560°C for 2 hours (b) heat-treated at 600°C for 2 hours and (c) heat-treated at 600°C for 2 hours.

particles at elevated temperatures include the removal of the contaminants, impurities, and absorbed water from the surface. This helps to form a clean and uniform protective layer of $SiO_2$.

The evolution of interfacial reaction products in the oxidized SiCp/2014Al composite after being heat treated at various temperatures is shown in Fig. 6a–c. In Fig. 6a nanoparticles were observed on the oxidized-layer of the particles heat treated at 560°C for 2 hours. The nanoparticles were identified as MgO according to the experimental results obtained by Zhang [6]. Fig. 6b and c showed the interfacial morphology of the composite heat treated at 600°C for 2 hrs. A mixture of $MgAl_2O_4$ crystals and Si were observed, which were similar to those observed from the $Al_2O_3$/6061Al composites [14]. A close examination clearly showed that clusters of octahedral $MgAl_2O_4$ crystals and Si have nucleated in the middle of the rim-shaped $SiO_2$ depletion basins. Fig. 7a shows the bright field TEM image of the SiCp/2014Al composite with oxidized particles heat-treated at 600°C for 2 hours. The interfacial reaction products, which were identified as $MgAl_2O_4$, Si, $\theta$-$CuAl_2$ phase by means of energy dispersive spectroscopy (EDS), convergent beam electron diffraction (CBED) pattern and electron diffraction pattern, are shown in Fig. 7b–7e. $MgAl_2O_4$ crystals were observed between $SiO_2$ layer and aluminum matrix, which confirmed the result from SEM observation. Fig. 7f shows the crystalline structure between the interfacial reaction product $MgAl_2O_4$ and SiC by observation of HRTEM.

Fig. 8a shows the interfacial reaction products of the extracted particles from the composites heat treated at 800°C for 1 hour. X-ray diffraction analysis of the extracted particles from the 2014Al composite revealed that the reaction products consisted of the mixture of $Al_4C_3$, $MgAl_2O_4$, and Si. This is shown in Fig. 8b and c. The appearance of $Al_4C_3$ crystals at the surface of oxidized-layer showed the depletion of $SiO_2$ layer, resulting from the excess interfacial reaction at elevated temperatures for extended holding time. Under such a condition, the interfacial reaction occurred continuously according to the reaction (1).

## 5. Discussion

Based on the TEM, SEM and X-ray diffraction observations, it is obvious that the pre-oxidation of SiC particles has a significant effect on the interfacial reaction characteristics. In the SiC/2014Al composite, $Al_4C_3$ can form from the reaction (1) between SiC and aluminum at elevated temperatures. The oxidized layer $SiO_2$ in oxidized SiC reinforced 2014 Al composite dissolved in the melt and is depleted by Mg and Al element during the reaction between $SiO_2$ and aluminum alloy containing Mg. Meanwhile, MgO, $Al_2O_3$, $MgAl_2O_4$, and

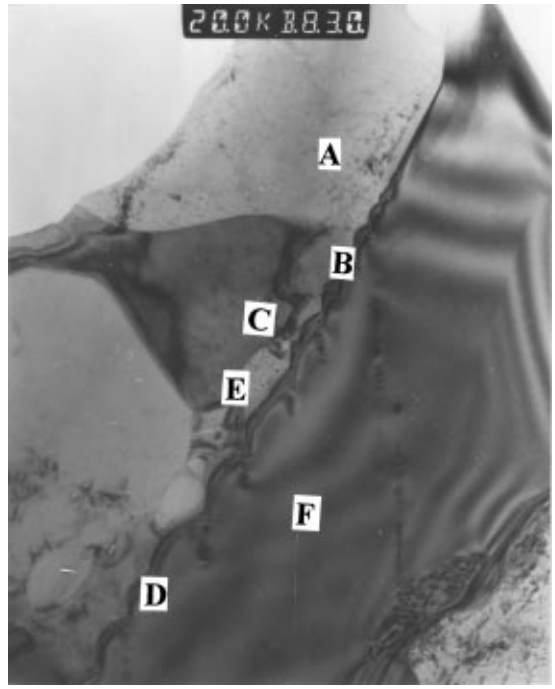


(a)

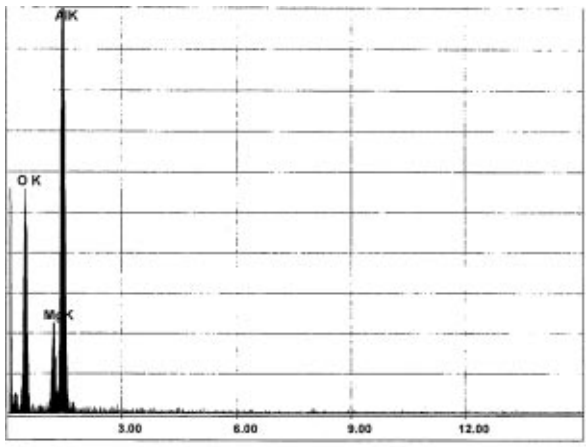


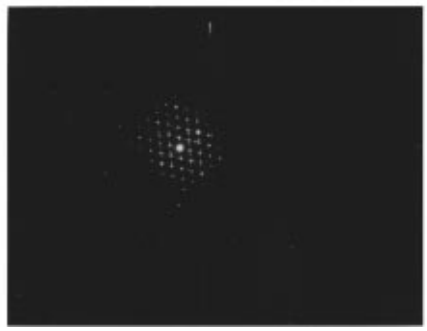

(b)

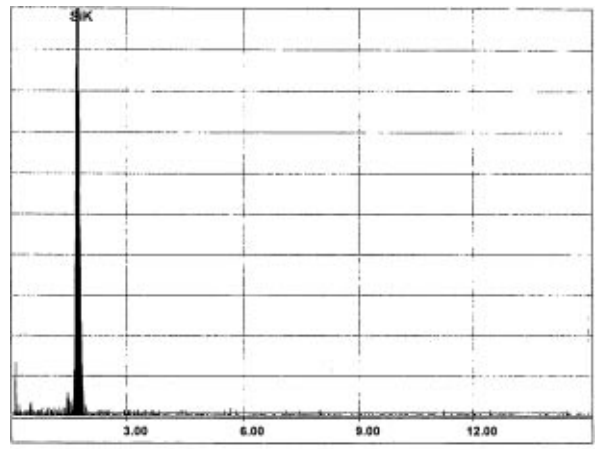


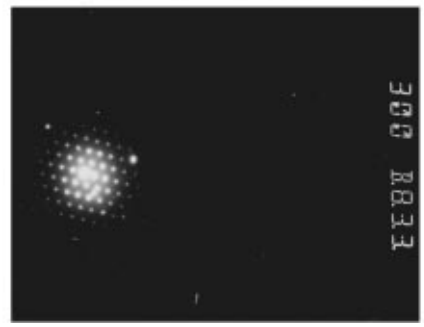

(c)

*Figure 7* TEM and HRTEM images showing the interfacial reaction products between oxidized SiC and 2014Al matrix (A: Al-matrix, B: $MgAl_2O_4$, C: Si, D: $SiO_2$, E: $\theta$-$CuAl_2$, F: SiC ) (a) TEM bright field image of the interfacial reaction products (b) EDS and electron diffraction pattern B-$MgAl_2O_4$ (c) EDS and electron diffraction pattern C-Si (d) EDS and CBED E-$\theta$-$CuAl_2$ (e) EDS A-Al-matrix (f) HRTEM images showing the fine microstructure of the interfacial reaction product $MgAl_2O_4$. (*Continued*).

$Mg_2Si$ may precipitate from the solution according to the following reactions:

$$4\langle Al\rangle + 3[SiO_2] \rightarrow 2[Al_2O_3] + 3\langle Si\rangle \quad (8.1)$$

$$2\langle Mg\rangle + [SiO_2] \rightarrow 2[MgO] + \langle Si\rangle \quad (8.2)$$

$$[MgO] + [Al_2O_3] \rightarrow [MgAl_2O_4] \quad (8.3)$$

$$\langle Mg\rangle + 2\langle Al\rangle + 2[SiO_2] \rightarrow [MgAl_2O_4] + 2\langle Si\rangle \quad (8.4)$$

$$2\langle Mg\rangle + \langle Si\rangle \rightarrow [Mg_2Si] \quad (8.5)$$

$$3\langle Mg\rangle + 4[Al_2O_3] \rightarrow 3[MgAl_2O_4] + 2\langle Al\rangle \quad (8.6)$$

Where $\langle\ \rangle$ and $[\ ]$ in the above equations correspond to species in the liquid and in the solid phases respectively in the melt.

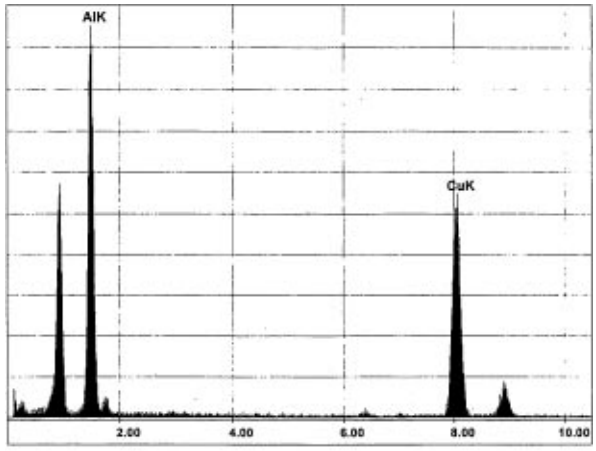


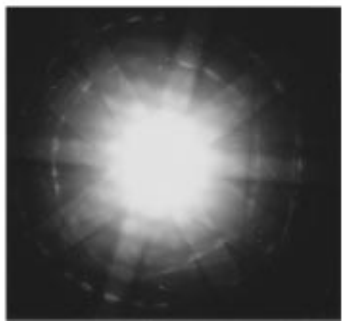

(d)

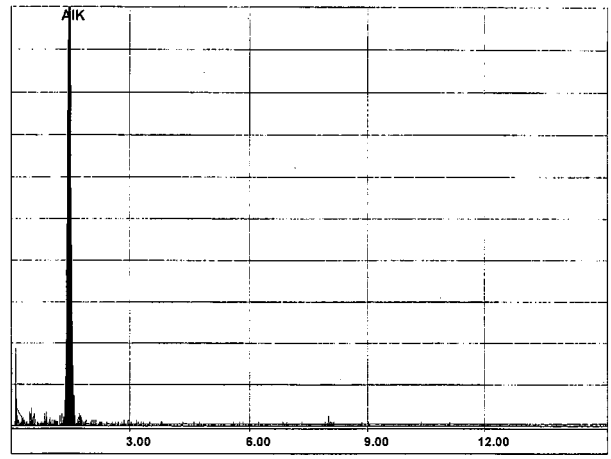


(e)

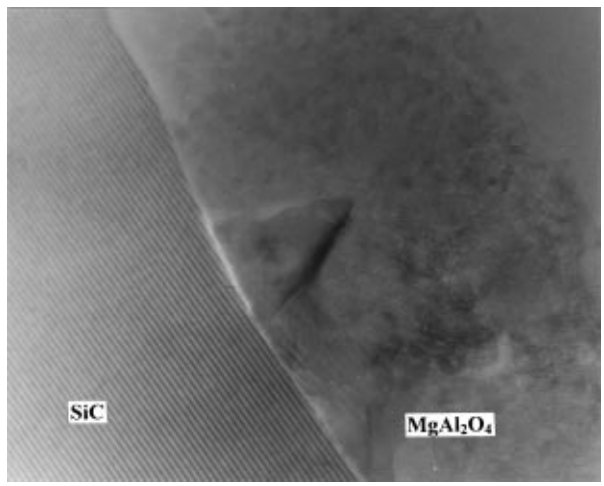


(f)

*Figure 7* (*Continued*).

There are a lot of reports on the interfacial characteristics and correlating reaction products in the composites [6, 7, 14, 18, 19]. Such as Gu *et al*. [7] found a concentration of aluminum within the interface of oxidized SiC by meansurement of EELS spectra which indicated that the above reaction (8.1) could occur between the oxidized layer of SiC particles and pure aluminum. Zhang *et al* [6] characterized the interfacail reaction products of oxidized-SiCp/Al-Mg (5083) composite by X-ray diffraction and TEM, from which the crystal boundaries of the MgO (or $MgAl_2O_4$) reaction products were believed to be the diffusion channels during the interfacial reactions. According to their results, the interfacial reaction takes place, followed by the above reaction equations (8.2) and (8.4). Lee *et al*. [14, 18] observed the interfacial reaction product octahedral shape $MgAl_2O_4$ in the $Al_2O_3$p/6061 composite by means of X-ray diffraction, SEM and TEM. However, in Lee's report, the particle was $Al_2O_3$ not oxidized-SiC and also the composition of matrix was different from the present composite. How will the interfacial reaction in the oxidized-SiCp/2014Al composite ever take place? There are no any reports to describe it details.

Comparing the morphologies between Fig. 6a, b, and c, the results clearly showed that nano-MgO particles were formed initially when the composite was heat treated above the solidus of aluminum alloy matrix. This is because Mg is an active element and it usually segregates at the interface. As the nano-size MgO is not stable at high temperatures for holding long time, it could react with aluminum alloy and be transformed

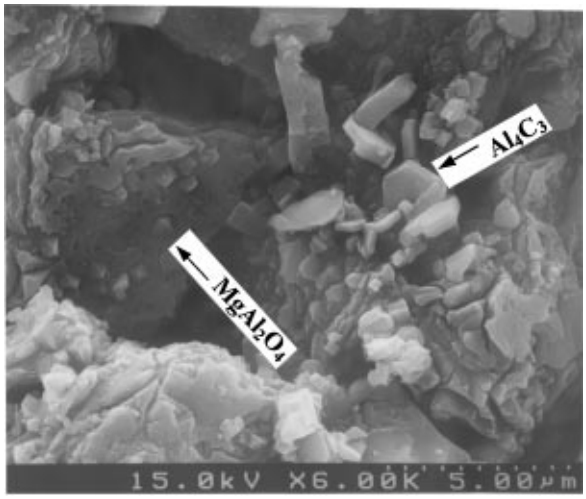


(a)

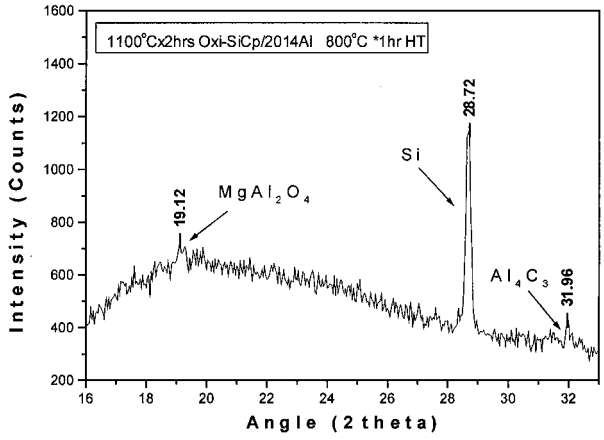


(b) $2\theta$ Angle range from 16∼33°

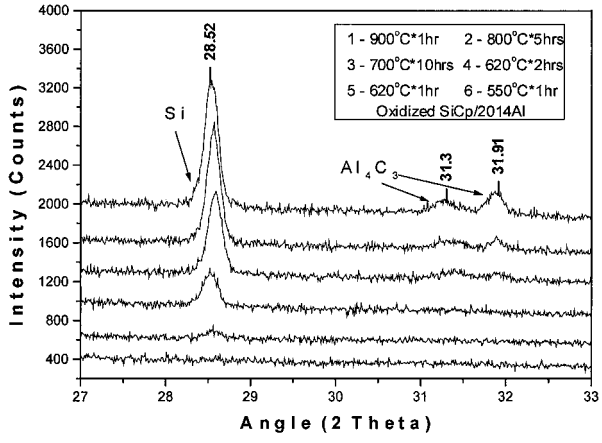


(c) $2\theta$ Angle range from 27∼33°

*Figure 8* SEM micrograph and X-ray diffraction profiles for electrochemically extracted SiC particles from oxidized-SiCp/2014Al composites heat treated at elevated temperatures samples: (a) SEM micrograph for the composite after heat treated at 800°C for 1 hour (b) X-ray diffraction for extracted particles from the composite after heat treated at 800°C for 1 hour (c) X-ray diffraction for extracted particles from the composite after heat treated at elevated temperatures.

into the stable octahedral $MgAl_2O_4$ crystal:

$$4\langle Al\rangle + 2[MgO] + 3[SiO_2] \rightarrow 2[MgAl_2O_4] + 3\langle Si\rangle \quad (9)$$

Thereby, the interfacial reaction between oxidized SiC particles and 2014 Al alloy will occur according to above chemical reaction equations (8.2) and (9). However, after the $SiO_2$ layer is completely consumed, Al will then react with SiC to form $Al_4C_3$ at the interface, shown in Fig. 8.

## 6. Conclusions

1. The passive-oxidized behaviors of as-received SiC particles have been studied, on the basis of the weight changes of the transformation from SiC into $SiO_2$. The dependence of the volume fraction of $SiO_2$ layer and their thicknesses on holding time show the parabolic trends at all temperatures investigated. The present oxidation data of SiC particles are available for the control of the oxidation parameters and the degree of oxidation for SiC particles.

2. Observation on the interfacial reaction between the oxidized SiC particles and 2014 aluminum alloy showed that nano-particles MgO can form initially but will eventually turn into a thermostable $MgAl_2O_4$ crystals.

3. Observation by HRTEM showed that the $SiO_2$ layer has a good bonding with both SiC and 2014Al matrix. However, it can be depleted by the interfacial reaction at elevated temperatures after extended thermal exposure.

## Acknowledgment

Zhongliang Shi is grateful for the supports from the National Nature Science Foundation of P.R. China grant No. 59631080 and the Science and Technology Policy Institute of Korea (STEPI) as a visiting scientist at Korea Institute of Science and Technology and Japan Society for the Promotion of Science as a JSPS fellow at Kyoto University.

## References

1. J. A. COSTELLO and R. E. TRESSLER, *J. Amer. Ceram. Soc.* **69** (1986) 674.
2. K. L. LUTHRA and H. D. PARK, *ibid.* **73** (1990) 1014.
3. B. SCHNEIDER, A. GUETTE and R. NASLAIN, *J. Mater. Sci.* **33** (1998) 535.
4. V. LAURENT, D. CHATAIN and N. EUSTATHOPOULOS, *Mater. Sci. Eng.* **A135** (1991) 89.
5. H. RIBES, M. SUERY, G. 'ESPERANCE and J. G. LEGOUX, *Metall. Trans.* **A21** (1990) 2489.
6. W. M. ZHONG, G. L'ESPERANCE and M. SUERY, *ibid.* **A26** (1995) 2637.
7. MINGYUAN GU, ZHI MEI, YANPING JIN and ZHENGAN WU, *Scripta Mater.* **40** (1999) 985.
8. R. Y. LIN, "Key Engineering Materials," edited by G. M. Newaz, H. Neber-Aeschbacher and F. H. Wohlbier, Vols 104–107, 1995, p. 507.
9. JAE-CHUL LEE, JI-YOUNG BYUN, SUNG-BAE PARK and HO-IN LEE, *Acta Mater.* **46** (1998) 1771.
10. JAE-CHUL LEE, HYUN-KWANG SEOK and HO-IN LEE, *Materials Research Bulletin*, **34** (1999) 35.
11. JAE-CHUL LEE, SUNG-BAE PARK, HYUN-KWANG SEOK, CHANG-SEOK OH and HO-IN LEE, *Acta Mater.* **46** (1998) 2635.
12. ZHONGLIANG SHI, TONGXIANG FAN, MINGYUAN GU, DI ZHANG and RENJIE WU, "Advanced Materials and Processing-PRICM 3," Hawaii, July, edited by T. W. Eagar *et al.*, 1998, p. 401.

13. TONGXIANG FAN, DI ZHANG, ZHONGLIANG SHI and RENJIE WU, *J. Mater. Sci*. **34** (1999) 5175.
14. J. C. LEE, G. H. KIM and H. I. LEE. *Mater. Sci. Tech*. **13** (1997) 182.
15. S. G. WARRIER, C. A. BLUE and R. Y. LIN, *J. Mater. Sci*. **28** (1993) 760.
16. S. G. WARRIER and R. Y. LIN, *ibid*. **28** (1993) 4868.
17. "CRC Handbook of Chemistry and Physics," 74th edition (CRC Press, 1992).
18. J. C. LEE, JUNG-ILL LEE and HO-IN LEE, *Scripta Mater*. **35** (1996) 721.
19. P. LU, R. E. LOEHMAN, K. G. EWSUK and W. G. FAHRENHOLTZ, *Acta Mater*. **47** (1999) 3099.

*Received 6 June*
*and accepted 15 November 2000*